

Test on an Optimized Cylindrical Non-contact Piezoelectric Actuator

Chen Heng¹, Chen Chao^{1*}, Yang Dong², Wang Junshan¹, Ge Yuyu¹

1. State Key Laboratory of Mechanics and Control of Mechanical Structure, Nanjing University of Aeronautics and Astronautics, Nanjing 210016, P. R. China;

2. China North Industries Group Corporation, Nanyang 473000, P. R. China

(Received 22 March 2016; revised 16 December 2016; accepted 31 December 2016)

Abstract: An optimization design for the cylindrical non-contact piezoelectric actuator is presented after analyzing the acoustic radiation pressure and acoustic viscous force. By adding the specific microstructure on the rotor to alter the near-field sound effect and maximize the use of high intensity acoustic field induced by the stator to drive the rotor, the rotor speed is increased. The finite element analysis of the acoustic field induced by a variety of rotors with different structures is conducted. A prototype is manufactured, the speed-test system for the actuator is built, and the driving characteristics are measured. The results suggest that the rotation speed of the rotor can reach 4 167 r/min, which demonstrates that the driving characteristics of cylindrical non-contact piezoelectric actuator are successfully improved using the optimization method proposed.

Key words: piezoelectric actuator; microstructure; finite element analysis; non-contact

CLC number: TN384

Document code: A

Article ID: 1005-1120(2017)01-0043-06

0 Introduction

Non-contact ultrasonic motor adopts fluid as an energy transfer medium between stator and rotor to avoid their direct contact^[1-2]. The research team led by Professor Sadayuki Ueha in Tokyo Institute of Technology, Japan, first presented the structure of liquid medium for ultrasonic motor, and by using water, salt water, and silicone oil as the medium of experimental prototype, they tested the ultrasonic motor in preliminary experiment^[3]. Hu et al. conducted experiments on the liquid flow phenomenon caused by cylinder vibrator. When the vibrator created axial wave, the liquid inside the cylinder would produce directional flow^[4-6]. By using the first-order irrotational and inviscid acoustic field, the acoustic stream could be obtained. Here, an optimization method is proposed to improve the speed of the cylindrical non-contact ultrasonic motor by spirally slotting the surface of the rotor in experi-

ments.

1 Structure of Cylindrical Non-contact Ultrasonic Motor

The traditional cylinder stator could only provide circumferential viscous force to drive the rotor's rotation instead of providing axial acoustic radiation force. With the support of the auxiliary organ, the rotor could be suspended absolutely. Thus the actuator consists of two parts: The piezoelectric ceramic transducer (PZT) transducer to supply suspension power and the cylinder rotor to restrict the rotor to rotate with a central position. The structure of the proposed cylindrical non-contact actuator is shown in Fig. 1, including a transducer, a rotor and a stator. The main function of the transducer is to produce the acoustic field on the upper surface by high frequency vibration, so that the rotor can be suspended above the transducer without touching it. If the

*Corresponding author, E-mail address: chaochen@nuaa.edu.cn.

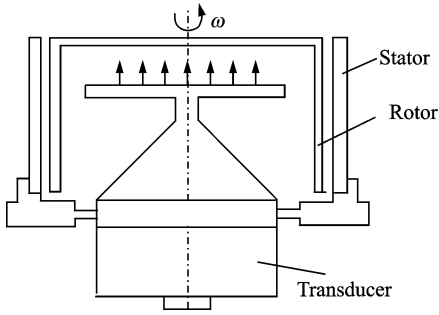


Fig. 1 Structure of non-contact actuator

PZT transducer did not work, the inner surface of the rotor would be in contact with the upper surface of the transducer because of the existence of gravity, and the rotor would not rotate due to the friction between the contact surfaces. When the transducer was working, its upper surface would be a radiating surface, thus generating acoustic suspension force between the transducer and the rotor. Since the whole system did not exert an axial pre-pressure on the rotor, the suspension force was equal to the gravity and the rotor could be suspended in a stable height. Here, the traveling wave generated by the stator's outer surface would be formed between the stator and the rotor, and the acoustic radiation force as well as the viscous force were thus realized. To achieve the cylindrical rotor's suspending and driving, different designs on the transducer and stator should be determined, and the finite element analysis too.

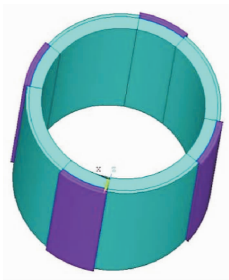


Fig. 2 Structure of stator

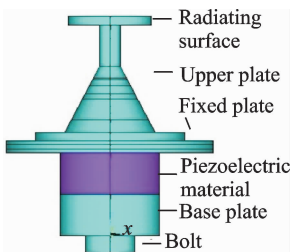


Fig. 3 Structure of PZT transducer

Figs. 2, 3 show the finite element model of the structure of the stator and the structure of the transducer, respectively.

2 Simulation on Output Characteristic Led by Motor Surface Structure

The non-contact ultrasonic motor which has a stator with smooth inner surface and a rotor with eight slots on the outer surface has been investigated first. Fig. 4 shows the distribution of sound field when the signal voltage is 100 V and the thickness of the air gap between stator and rotor was 50 μm . In Fig. 5, the acoustic pressure of the air layer (gap) between the stator and rotor increases when the voltage increases, and the value of the acoustic pressure is proportional to voltage. With the increase of the thickness of the slots, the acoustic pressure can be reduced, as well as the driving force and the rotor's maximum speed. Comparing the following images, it can be found that the sound pressure of copper is smaller than that of aluminum.

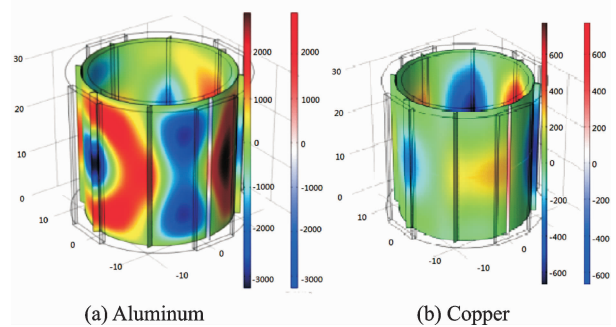


Fig. 4 Distribution of sound field (rotor with 8 slots)

In this study, we made 8, 12 and 16 slots on the rotor, respectively. The outer surface shape of the rotor is shown in Fig. 6, where R is the rotor diameter, r the inner diameter of the rotor, and d , α are the depth and the angle of the slots, respectively. To facilitate the processing, we define α as 90° .

The distribution of acoustic field in the air layer between the stator and the rotor is analyzed, respectively. To obtain the change of acoustic field in the gap, the thickness of air layer (gap) varied firstly. Subsequently, the rotors with different slot numbers are tested to deter-

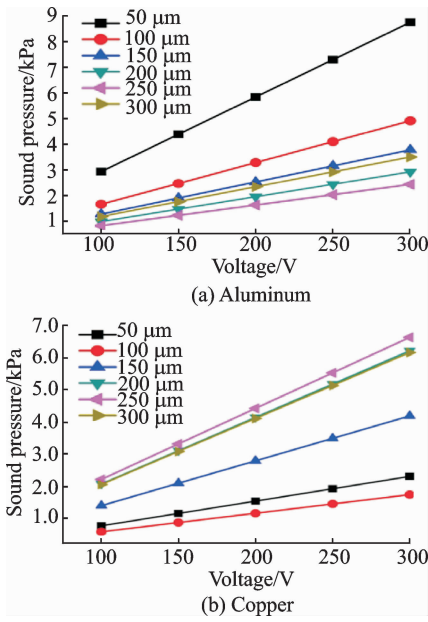


Fig. 5 Relationship between sound pressure and load voltage

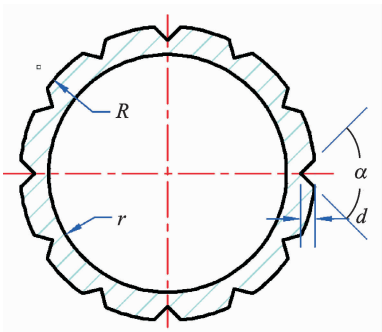


Fig. 6 Cross section of vertical slot rotor

mine how many slots are optimal in driving the rotor. Finally, the following conclusions could be obtained.

As shown in Fig. 7, the sound pressure in the slot increases with the increase of load voltage. When the slots between the stator and the rotor are larger than 150 μm, the sound pressure is close to that of the rotor with 8 slots. In the same slot thickness, the sound pressure in 8 slots is higher than those in 12 and 16 slots.

The calculation model is mainly composed of the cylinder types of the stator and the rotor. The gap between the stator and the rotor is of micron scale (50—300 μm). Since the air layer thickness is very small, we assume that the gas in the air layer, the inner surface of the stator and the rotor's outer surface form a relatively closed system when the actuator is working. The gas in the gap

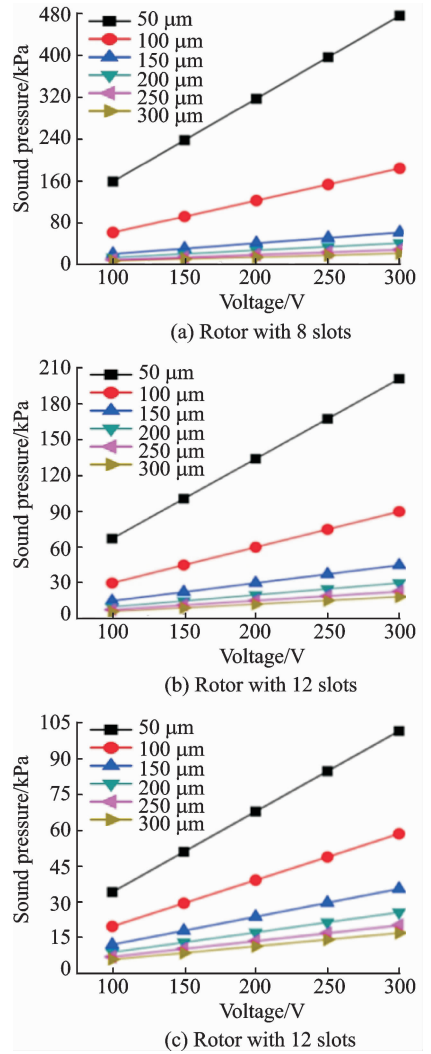


Fig. 7 Relationship between sound pressure and load voltage

exchanges nothing with the outside world in the rotating process of the rotor. In other words, the gas in the gap between the stator and the rotor does not form a stable air flow to drive the rotor's rotation. To tackle this problem, a novel method for slotting on the external surface of the rotor is put forward, as shown in Fig. 8. By adding spiral slots on the surface of the rotor, high pressure gas between the stator and the rotor can convect with the low pressure gas outside.

The equation of the spiral is

$$\begin{cases} x = r \cdot \cos(t + \alpha) \\ y = r \cdot \sin(t + \alpha) \\ z = b \cdot t \end{cases}$$

where r is the base circle radius, b the length of the lead, t the circumferential angle, and α the phase of the spiral starting point on the base circle at the bottom.



Fig. 8 Rotor structure with spiral slot

Here, the spiral's lead length is set as being equal to the height of the rotor. By adjusting the base circle radius to control the depth of the spiral slot, the starting point of the spiral line is determined by controlling the value of α . To compare the differences of the sound field in the air layer between the stator and rotor with different number of spiral slots, the numbers of spiral slots are chosen as single, double and four.

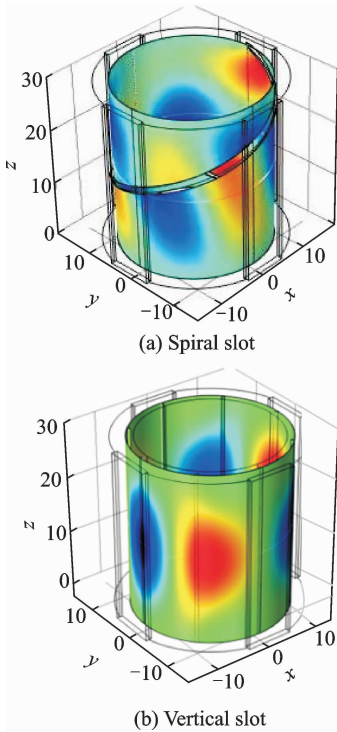


Fig. 9 Distribution curve of sound field

As shown in Figs. 9, 10, the acoustic field distribution of the gas layer with rotor having vertical slots is uniform but disturbed by the spiral slot. During the spiral rising process, both positive pressure and negative pressure distribution appear on both sides of the spiral slot. The sound pressure distribution along the direction of spiral is different from the periodic distribution

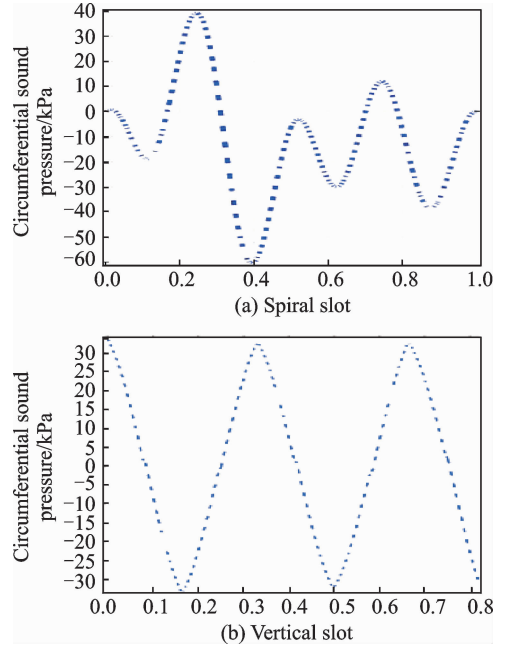


Fig. 10 Sound field-sound pressure curve

and the curve becomes more clutter. After the comparison of the results, it was not hard to conclude that the spiral slots change the sound pressure more obviously, and the driving effect on rotor is more efficient.

3 Experiment on Output Characteristic of Motor Influenced by Surface Structure

As shown in Fig. 11, the computer control system is comprised of laser displacement sensor, signal generators, power amplifier, monitor, laser head and actuating device. Two signal generators and power amplifier are used to drive the non-contact ultrasonic motor. Two sets of output signals with phase difference of 90° are connected with the power amplifier. Received the amplified signals, the stator thus generates a traveling wave and the rotor rotates. According to the periodic displacement relationship of the laser displacement sensor, the speed of the rotor can be calculated.

Rotation speeds with aluminum stator and copper stator were tested in the speeding test system, respectively. Due to the fact that the machining precision was uncontrollable, we cannot control precisely the gap thickness of $50 \mu\text{m}$ between

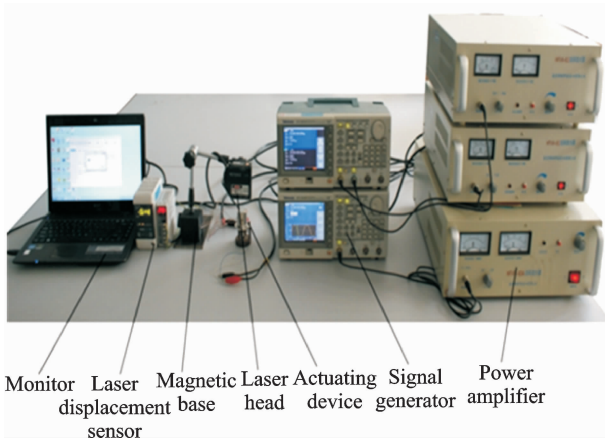


Fig. 11 Speed test system

the stator and the rotor, and the roughness of the surface would also affect the rotation speed. Therefore, we reduced the gap's thickness as much as possible and chose the stator with the best rotation effect.

Fig. 12 demonstrates the speed of the aluminum smooth surface stator driving slotted rotor. Fig. 12(a) shows the corresponding relationship between speed and driving signal frequency at different gaps. Fig. 12(b) gives the rotor with different number of slots when the gap thickness is $75 \mu\text{m}$. When the number of slots is 12, the rotor speed is higher. And from Fig. 13, we obtain the relationship between the rotor speed and frequen-

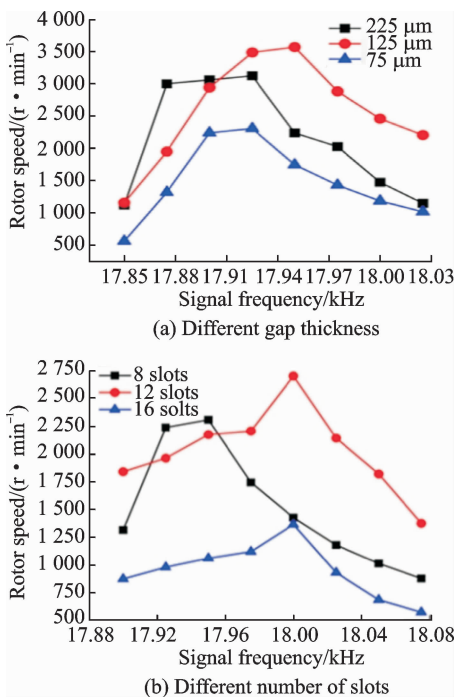


Fig. 12 Rotor speeds of aluminum stator

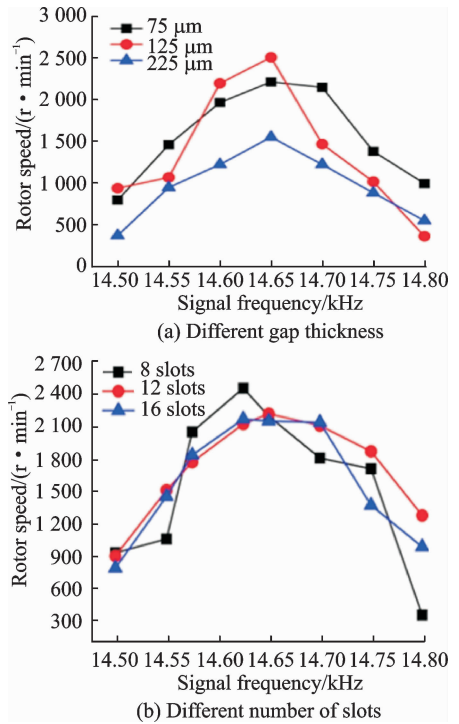


Fig. 13 Rotor speed of copper stator

cy of the copper stator. In the previous simulation, we obtained the maximum speed of the rotor when the number of slots reached 8 and the gap thickness is $100 \mu\text{m}$. Here the results of the experiments are consistent with those of the simulation. Comparing the copper and aluminum stators, it is found that the aluminum stator perform better in driving rotor, but not obviously. Since the processing of aluminum stator is more difficult than that of copper one, the copper stator is adopted in this study.

After that, we carried on experiment to investigate the driving characteristics of the rotor with a single spiral slot, as well as double and four slots, respectively. We set the gap thickness $150 \mu\text{m}$, and the loading signal voltage was up to 220 V.

Fig. 14 shows the results of experiment on the rotor with different number of spiral slots and the stator was made of copper. The gap thickness was $150 \mu\text{m}$ and the signal voltage was 220 V. From Fig. 14, the following conclusions can be drawn. The maximum speed of the rotor is 4 167 r/min after adding spiral slots on the surface of the rotor's outer surface, which is considerably higher than that with vertical slots. It is

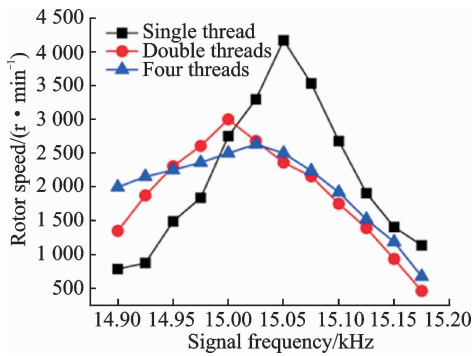


Fig. 14 Relationship between rotor speed and driving frequency

shown that the spiral microstructure effect on the promotion of the rotor speed is obvious. The result is obtained with the driving peak-peak voltage of 300 V. If we increase the amplitude of driving voltage, the rotor speed will soar. Among all the rotor's spiral surface microstructures, the effect of a single spiral slot is the best, while that of the four spiral slots is the worst.

4 Conclusions

Taking the structure characteristics of non-contact ultrasonic motor and driving principle into account, the generating mechanism of acoustic streaming in the air layer between stator and rotor is analyzed theoretically. The microstructure on the outer surface of the rotor is optimized by theoretical analysis and simulated using the finite element software. In addition, the driving characteristics are also investigated by experiments. Finally, the structure of the rotor's surface is determined and a prototype is manufactured. A non-contact testing speed system is built and the driving characteristics are tested. It can be found that the measured rotor's speed nearly doubles after optimization. The result shows that when the non-contact cylindrical piezoelectric actuator for a rotor having spiral microstructure on the surface, its driving performance has been significantly improved.

Acknowledgements

This work was supported by the National Basic Research Program of China ("973" Program) (No. 2015CB057500), the National Natural Science Foundation

of China (No. 11174149), the Fundamental Research Funds for the Central Universities (No. NJ20140024), and State Key Laboratory of Mechanics and Control of Mechanical Structures Research Fund (No. MCMS-0312G02).

References

- [1] XIA Changliang, HU Junhui, SHI Tingna, et al. Study on theory and experiment of non-contact type ultrasonic motor with fluid medium[C]//Proceedings of the CSEE. [S.l.]:[s.n.],2001:64-67.
- [2] JI Ye, ZHAO Chunsheng. Cylinder type non-contact ultrasonic motor[J]. Journal of Nanjing University of Aeronautics & Astronautics, 2005, 37(6):690-693. (in Chinese)
- [3] MAENO T, TSUKIMOTO T, MIYAKE A. Finite-element analysis of the rotor/stator contact in a ring-type ultrasonic motor [J]. Ultrasonic, Ferroelectrics and Frequency Control, IEEE Transactions on, 1992, 39(6): 668-674.
- [4] HU Junhui, NAKAMURA K, UEHA S. Optimum operation conditions of an ultrasonic motor driving fluid directly[J]. Japanese Journal of Applied Physics, 1996, 35(1): 3289-3294.
- [5] YAMAZAKI T, HU Junhui, NAKAMURA K, et al. Trial construction of a noncontact ultrasonic motor with an ultrasonically levitated rotor[J]. Japanese Journal of Applied Physics, 1996, 35(5): 3286-3288.
- [6] HU Junhui. Analyses of an ultrasonic motor driving fluid directly[J]. Japanese Journal of Applied Physics, 1995, 34(5B):2702-2706.

Mr. **Chen Heng** is a Ph. D. candidate in State Key Laboratory of Mechanics and Control of Mechanical Structure of Nanjing University of Aeronautics and Astronautics (NUAA). His research interests include machine design, Mechanical manufacturing technology, piezoelectric actuator design and application.

Dr. **Chen Chao** is a professor in State Key Laboratory of Mechanics and Control of Mechanical Structure, at NUAA. He received his Ph. D. degree in NUAA. His research interests include machine design, Mechanical manufacturing technology, piezoelectric actuator design and application.

Mr. **Yang Dong** is an engineer at China North Industries Group Corporation in Nan Yang. He received his M. S. degree at North University of China. His research interests are machine design and manufacturing.

Mr. **Wang Junshan** is a Ph. D. candidate in State Key Laboratory of Mechanics and Control of Mechanical Structure of NUAA. His research interests include machine design, Mechanical manufacturing technology, piezoelectric actuator design and application.

Mr. **Ge Yuyu** is an engineer at Jiangsu CRRC Electric Co., LTD. He received his M. S. degree in NUAA. His research interests are piezoelectric actuator design and application.